Climate adaptation for a natural atoll island in the Maldives - predicting the long-term morphological response of coral islands to sea level rise and the effect of hazard mitigation strategies

F. E. Roelvink[1,2*], G. Masselink[1], C. Stokes[1], and R. T. McCall[2]

[1]School of Biological and Marine Sciences, University of Plymouth, Plymouth PL4 8AA, UK

[2]Deltares, Boussinesqweg 1, 2629 HV Delft, The Netherlands

Corresponding author: Floortje Roelvink (floortje.roelvink@deltares.nl)

Key Points:

- The natural island of Fiyoaree (Maldives) is projected to keep pace with 0.5m sea level rise by 2100 through morphological adjustment.
- Ignoring the long-term morphological response of Fiyoaree to sea level rise triples the predicted extreme overwash events by 2100.
- Reef adaptation measures reduce the inshore wave energy, limiting vertical accretion but often mitigating the impact of extreme events.

Abstract

Coral atoll islands, common in tropical and subtropical oceans, consist of low-lying accumulations of carbonate sediment produced by fringing coral reef systems and are of great socio-economic and ecological importance. Previous studies have predicted that many coral atoll islands will become uninhabitable before the end of this century due to sea level rise exacerbating wave-driven flooding. However, the assumption that such islands are morphologically static, and will therefore 'drown' as sea levels rise, has been challenged by observations and modelling that show the potential for overwashing and sediment deposition to maintain island freeboard. However, for sustainable habitation, reliable predictions of island adjustment, flooding frequency and the influence of adaptation measures are required. Here, we illustrate the effect of various adaptation measures on the morphological response of an atoll island to future sea level rise using process-based model simulations. We found that the assumption of a static island morphology leads to a significant increase in the predicted frequency of future island flooding compared to morphodynamically active islands, and demonstrate that natural morphological adjustment is a viable mechanism to increase island freeboard. Reef adaptation measures were shown to modify the inshore wave energy, influencing the equilibrium island crest height and therefore the long-term morphological response of the island, while beach restoration mainly delays the island's response. If embraced and implemented by local communities, allowing for natural island dynamics and implementing well-designed adaptation measures could potentially extend the habitability of atoll islands well beyond current projections.

Plain Language Summary

Low-lying coral atoll islands, protected by coral reefs, may become uninhabitable due to frequent flooding as sea levels rise. However, studies also show that if left undisturbed by human activity, these islands could grow vertically through the process of sand being deposited on the islands by waves washing over them. Understanding how these islands will change and the impact of actions like coral reef restoration is crucial for planning sea level rise adaptation. In this study, we used a computer model to see how an island in the Maldives will respond to different sea level scenarios and adaptation measures. We found that if we assume that the island does not change over time, we will predict far more flooding in the future than if we allow the island to adjust naturally to sea level rise. We also found that some adaptation measures can reduce the damage from large waves that can lower and flood the island, while further damage to the coral reefs can lead to more flooding. The results of the study show that allowing the natural dynamics of coral atoll islands to take place may allow island communities to stay on their islands longer than we thought.

1 Introduction

Atoll islands occur in the tropics and are wave-built accumulations of carbonate sediment derived from the decomposition of calcium carbonate-secreting organisms that dwell on the adjacent, ring-shaped coral reef system. The islands are of great socio-economic and ecological importance. They are the only naturally habitable land in atoll nations such as Maldives, Tuvalu, Kiribati and the Marshall Islands, and in atoll island groups such as Chagos and Lakshadweep. With a combined population of c. 1 M, atoll islands rely heavily on tourism for their GDP. They also provide a critical habitat for diverse endemic and some threatened species (e.g., green turtles).

A characteristic feature of atoll islands is their low-lying nature (often < 1-2 m above high tide level), which makes them vulnerable to coastal flooding and island inundation during extreme events (e.g., cyclones, storm surges, tsunamis). Model-based projections of global mean sea level rise (SLR) by 2100 suggest an indicative range of 0.44–0.76 m SLR under the SSP2-4.5 ("middle of the road" Shared Socioeconomic Pathway) emission scenario (*IPCC, 2021*). SLR will significantly increase the risk of flooding, particularly in the tropics, where even a 5-cm SLR has been shown to double the exceedance probability of the 50-yr water level (*Vitousek et al., 2017*). It is widely acknowledged that atoll islands are amongst the most vulnerable (coastal) environments to climate change and it has been predicted that most of them will be uninhabitable by the mid-21st century due to SLR exacerbating wave-driven flooding (*Storlazzi et al., 2018*).

Predictions of the impact of SLR on atoll islands are generally based on the application of process-based hydrodynamic models (e.g., XBeach; *Roelvink et al., 2009*). Such models show overall good performance in characterizing water levels and wave transformation over the reef, and correctly predict the increase in wave energy along atoll island shores due to the elevated water depths on the reef platform (*Beetham and Kench, 2018*; *Jennath* *et al., 2021*). These models can also account for the increase in flood risk due to reduced roughness of the reef platform resulting from coral reef degradation (*Quataert et al., 2015*) due to local anthropogenic stressors (overfishing, pollution) and global climate stressors (increase in ocean water temperature, ocean acidification). They can also be used to assess the potential flood reduction from nature-based solutions such as coral restoration (*Roelvink et al., 2021*).

Simulations of island flooding and inundation in response to sea level rise generally assume that the island itself does not respond morphologically (i.e., by changing its shape or elevation). However, this is an oversimplification, as atoll islands can adjust to rising sea levels by increasing their elevation as a result of waves overwashing the island, transporting sediment from the reef platform and front of the island onto the top of the island. In fact, geological studies argue that higher sea levels and associated high-energy wave events are actually critical for island initiation and may even facilitate further vertical reef island building, provided there is an adequate sediment supply (*East et al., 2018*). Depositional overwash processes have been observed *indirectly* on atoll islands through post-storm surveys (*Smithers and Hoeke, 2014; Duvat and Pillet, 2017*) and *directly* through small-scale physical modelling (*Tuck et al., 2019a; Tuck et al., 2019b; Tuck et al., 2021*). These experiments have been corroborated by numerical modelling (*Masselink et al., 2020; 2021*) and demonstrate that repeated overwash occurring under high wave and/or water level conditions can enable an atoll island to keep pace with SLR. Whether an atoll island can maintain its freeboard (defined here as the difference between island crest elevation and mean sea level; *EurOtop, 2018*) during rising sea levels, is influenced by a number of factors, including the rate of SLR, storm wave climate and sediment supply.

Allowing atoll islands to vertically accrete in response to SLR has significant implications for the assessment of future coastal risk and results in less pessimistic predictions of future island habitability (*Masselink et al., 2020*). In fact, provided there is sufficient sediment supply to the island and the flooding regime is not too frequent and hazardous, island habitability is potentially sustainable. However, for communities to continue to occupy an atoll island that is naturally adjusting to SLR through overwash-induced accretion demands flexibility and adaptability from the current island infrastructure and communities, and a departure from the construction of hard-engineered structures, as these prevent waves from overwashing and the island from morphodynamically adjusting (*Kench, 2012*; *Brown et al., 2020*). Constraints to living on such a naturally-adjusting island are also considerable and include, amongst others, lack of space for the island to migrate to, resilience of island communities to episodic and potentially hazardous flood events, adaptability of current island infrastructure and housing, threats to fresh water supply and adverse impacts on agriculture. At the same time, early-warning systems (*Winter et al., 2020*) and nature-based coastal protection measures (*Barnett et al., 2022*) can help facilitate island communities to sustainably live on a dynamic and frequently-flooded island.

Adaptation measures, including nature-based solutions such as reef restoration and enhancing beach vegetation, may help atoll islands to gradually adjust to SLR. However, quantifying the effectiveness of these measures requires process-based, long-term morphodynamic modelling. Currently, an approach for such long-term process-based morphodynamic modelling is lacking. XBeach is typically used to resolve complex hydrodynamic processes on reefs (*Lashley et al., 2018; Quataert et al., 2020*) and the morphodynamic response during (a few) storm events (*McCall et al., 2015; Masselink et al., 2020*), but is often considered computationally prohibitive for modelling longer time scales. Conversely, wave-averaged models such as Delft3D are used to simulate long-term (longshore) coastal evolution (*Luijendijk et al., 2019*), but lack second-order (low-frequency) wave dynamics, which tend to dominate during overwash and flooding events.

Here, we use a small island (Fiyoaree) located on the exposed rim of Huvadhoo Atoll in the Maldives as a case study to develop an efficient approach for investigating future atoll island habitability. Based on 40 years of modelled wave data (ERA5) and measured water level data, we first generated an 80-year future synthetic wave and water level time series. Wave events were filtered using an XBeach-based metamodel (BEWARE; *Pearson et al., 2017*) to focus on only those events with significant expected morphological change. The cross-shore morphodynamic development of the island was then modelled using the phase-resolving XBeach model. The morphological response of the island and the changes in flood characteristics were compared for different adaptation strategies.

Section 2 describes the study site, elaborates the six-step approach for developing future wave and water level time series, and describes the numerical model setup for assessing the morphological response of the island. Section 3 then describes the wave transformation across natural and adapted reef profiles (Section 3.1), the morphological response of natural coral islands (Section 3.2) and how adaptation measures influence the morphological response (Section 3.3).

2 Materials and Methods

2.1 Site description

This study focuses on the populated island of Fiyoaree (c. 1,500 people) at the SSW rim of the Huvadhoo Atoll, directly exposed to waves approaching from SE to NW. The island is approximately 1.6 km long and 0.6 km wide and is fronted by a 100–200 m wide reef flat (see Figure 1a). The shallow reef flat is covered with alternating patches of sea grass, sediment capturing sponges, and, among others, porites corals. The reef crest at the edge of the reef flat is clearly defined and features a wide variety of coral types, such as acropora, heliopora, and platygyra. The fore reef is composed of large spur (shore-normal ridge of coral) and groove (shore-normal channels) formations, with maximum spur heights near the reef crest of up to 3 m above the adjacent groove and alongshore wavelengths of 10–15 m (see Figure 1d). Like many islands on the southwestern rim of the Huvadhoo Atoll, Fiyoaree is composed of a mixture of sand, gravel, and cobble-size material. Most of the ocean beach is lined with a conglomerate platform composed of coral fragments, located around the mean sea level.

Water level variations due to tide and non-tidal residuals (NTR) are relatively low for the Maldives. The microtidal regime (tidal range less than 2 m) is semidiurnal with strong diurnal inequalities. At Gan, the nearest tide gauge located 100 km south of Fiyoaree, the mean spring tidal range is 0.96 m (*Wadey et al., 2017*). The NTR primarily contains the meteorological contribution to sea level (surge). Wind-driven surge levels are low for Huvadhoo Atoll since the atoll is located near the equator and therefore outside the normal range of cyclone activity. Furthermore, wind-driven surge levels are generally low for the steep coastlines of coral islands. For steep coasts, and especially outside the range of cyclones, the inverse barometer effect is generally the main contribution to total surge (*Van Ormondt et al., 2021*).

The wave climate of the Maldives is characterized by remotely generated swell waves, with largest significant wave heights accompanied by peak periods of 10–12 s and up to 24 s (*Amores et al., 2021*). Persistent low-pressure systems south of the Maldives (between 40 and 50 degrees south) generate year-round southwestern swells with maximum significant wave heights of 4 m (*Amores et al., 2021*). During the southwest monsoon (May to November), strong winds from the south to southwest generate long period and large swell waves (*Wadey et al., 2017*), as well as shorter period sea waves. Fiyoaree is relatively sheltered from the northeasterly waves generated during the northeast monsoon (November to April) but is fully exposed to the southwest swell.

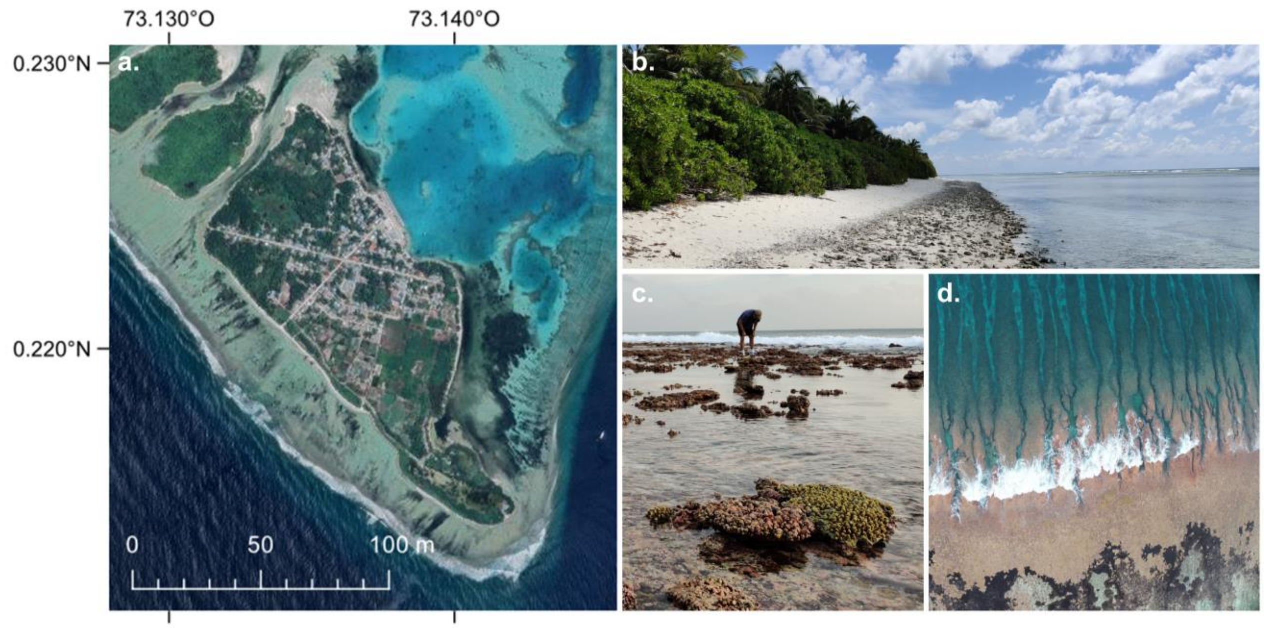

Figure 1: Map of Fiyoaree Island on Huvadhoo Atoll (panel a) and photographs of the beach (panel b), reef crest (panel c), and spur and groove system (panel d).

2.2 Generating forcing conditions

To assess how coral islands morphologically adjust to SLR (Section 2.3), we need a realistic future time series of wave conditions and water levels to force the morphodynamic model. While it is impossible to predict the exact sequence of future waves and water levels that will occur, the statistical characteristics of the past wave and water level climate can be used to generate multiple feasible realizations of the future time series. This time series can be used to force the XBeach model to generate a single feasible deterministic morphological prediction, or probabilistic predictions where computational effort allows. We describe the future wave and water level time series by a sequence of synthetic wave events, parametrized by the signifcant wave height H_s, the time evolution of H_s during the event, the peak wave period T_p, mean wave direction, storm surge and duration. A combination of advanced statistical techniques was used to generate reliable and realistic time series for the next 80 years (2020–2100). The method for deriving synthetic wave events involves six main steps (see Figure 2), as elaborated in the following sections.

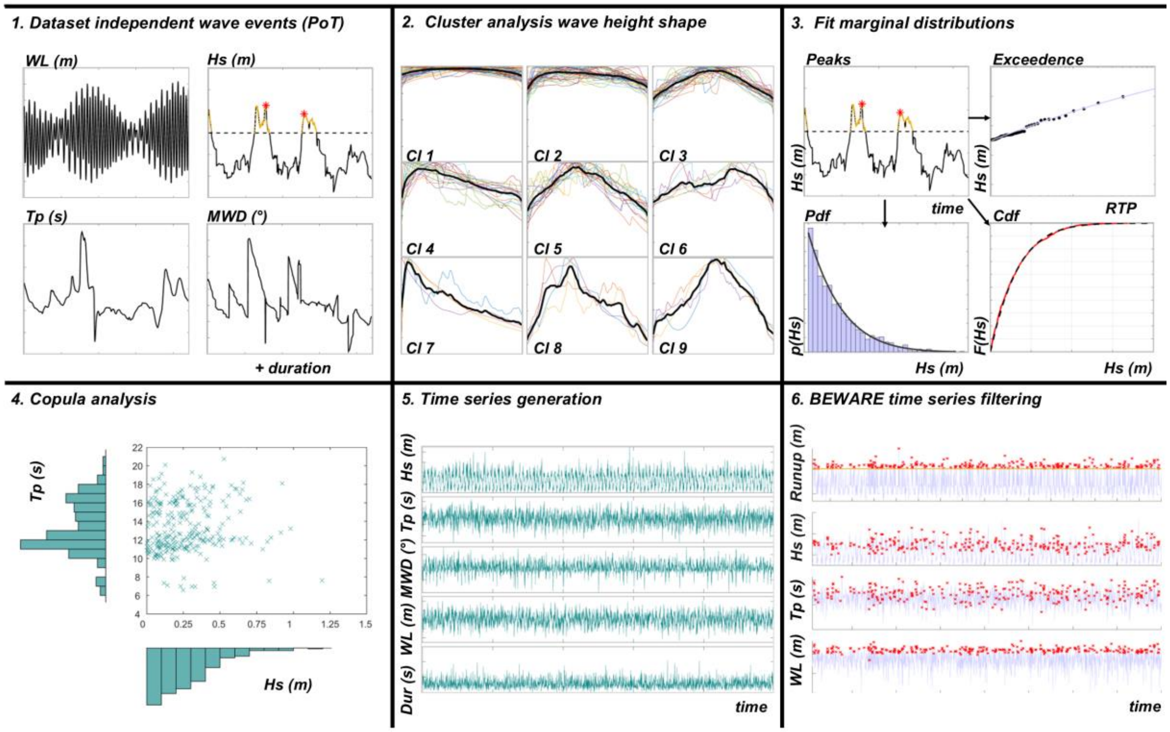

Figure 2: Overview of the methodology to obtain an 80-year time series of wave and water level conditions to efficiently force a morphodynamic model.

Step 1 – Obtain a dataset of independent wave events

Water levels were obtained from water level measurements at the Gan tide gauge over the period 1992–2018. The water level times series was detrended and was then raised to the current mean sea level to correct for sea level rise. Non-tidal residuals are a function of various oceanographic and/or meteorological effects (e.g., wind, barometric pressure, temperature, El Niño/La Niña effects) and were obtained by subtracting predicted tide levels from the detrended water level measurements. Wind and wave climate variables were obtained from the ERA5 dataset (*Hersbach et al., 2020*) from the European Centre for Medium-Range Weather Forecasts (ECMWF), which contains hourly estimates of various atmospheric, land and oceanic climate variables. The wind and wave data are available on a global grid with a resolution of 0.25 and 0.5 degrees, respectively, and cover the period from 1979 to the present. ERA5 wave data have been extracted from the output node closest to Fiyoaree (0° N, 72.5° E). Table 1 shows the resulting monthly mean and 99 percentile wave heights for the four distinct wave seasons identified by *LAMER (2013)*.

Table 1: Wave conditions at Fiyoaree summarized from the analysis of ERA5 wave data at coordinates 0° N, 72.5° E.

	Northeast (NE) monsoon	**Transition Period 1**	**Southwest (SW) Monsoon**	**Transition Period 2**
Period	December–February	March–April	May–September	October–November
Short wave direction	E-NE	NE-SE	S-SW	W
Swell wave direction	S-SW	S-SW	S-SW	S-SW
Mean significant wave height per month	1.3	1.3–1.4	1.8–1.9	1.4–1.6
99 percentile significant wave	1.7–2.0	1.8–2.2	2.5–2.6	2.4–2.5

height per month

The peaks-over-threshold (PoT) method was used to identify individual wave events based on wave height peaks and a minimum duration between events. The wave time series was first divided into four distinct wave seasons (see Table 1) to accurately represent the seasonal and monsoonal-driven variations in the wave climate of the Maldives. The threshold for the POT method was defined as the mean plus one standard deviation of H_s, which equates to a threshold at the 68.3 percentile level, in line with *Masselink et al. (2014)*. Note that although this threshold is relatively low, it allows the inclusion of shorter return period events that may be relevant to the morphological development of coral islands. Wave height peaks were identified using a minimum threshold of 12 hours between peaks to ensure that selected peaks originate from independent events. Durations were defined as the time interval associated with the wave height time series intersecting with the wave height threshold. This allows not only for the description of the peak H_s, peak T_p, and non-tidal residual water levels, but also of their evolution during an event.

Step 2 – Identify the wave height shape from cluster analysis

The events obtained in Step 1, each described by time series of wave conditions and the corresponding water levels, were parametrized for fitting marginal distributions (Step 3) and Copula (Step 4). Typically, wave events are characterized by key parameters including the maximum wave height and the corresponding wave period and direction during the event, as well as the duration. In addition to these parameters, we examined how wave heights and periods change throughout an event. Consistent shapes were evident for H_s over the duration of the event, but temporal variations in T_p were erratic, most likely reflecting a bimodal wave climate with peak periods alternating between wind wave and swell periods. The most common shape of T_p was found to be almost constant and was therefore adopted here. The evolution of H_s was parametrized by a single shape parameter using the k-means algorithm (*Lloyd, 1982*), which partitions a data set into groups with similar characteristics. The number of wave height shapes was optimized using the Silhouette index (*Rousseeuw, 1987*).

Step 3 – Fit marginal distributions to the variables

Optimized marginal distributions were fitted to the resulting dataset of variables to provide a statistical description of the wave events, for each wave season separately. The marginal distributions were optimized using the AIC criterion, a relative measure of how well a statistical model fits the data set from which it was generated (*Akaike, 1974*). The Generalized Pareto (GP), Generalized Extreme Value (GEV), Exponential, Weibull, and Rayleigh distributions were evaluated for their goodness of fit. The significant wave height (Weibull), mean wave direction (GEV), storm surge (Weibull), duration (Weibull), and wave height shape (Exponential) were well described by the above distributions. Standard unimodal marginal distributions were less adequate to describe the bimodal or even trimodal wave period shape but were chosen for their simplicity.

Step 4 – Describe the interdependence between variables using Copula

Copula analysis was used to establish the interdependence between pairs of variables for each wave season, linking the wave height to each different variable. Copulas mathematically link random variables described by different marginal distributions (*Nelsen, 2007*). Describing this dependency is important for accurately representing future wave scenarios, as variables (e.g., wave height and wave period) can be strongly linked (*Poelhekke et al., 2016*). The Frank copula family shows the best fit for most variable pairs, while the Gumbel copula was used to describe the link between wave height and period.

Step 5 – Generate synthetic wave events

Synthetic wave events were generated by sampling the variables from the marginal distributions and copula descriptions. The number of events in a given year and season was sampled from the historical number of events per season. The events were then randomly distributed within each season to define the corresponding tidal water levels. Ten synthetic wave event time series were generated, whose statistics fit well with the original data. A single time series was randomly selected for further modelling efforts due to computational limitations. An SLR of 0.5 m by 2100 at a constant rate of 6.25 mm/yr was assumed, representing the median prediction for an intermediate greenhouse gas (GHG) emission scenario (SSP2-4.5). The corresponding sea level rise values were added to the offshore water level.

Step 6 – Input reduction using BEWARE for efficient modelling

For computational efficiency, the input conditions for the XBeach morphodynamic simulations (see Section 2.3) were filtered using BEWARE2. BEWARE2 is an extension of the BEWARE (*Pearson et al., 2017*) wave runup metamodel for coral reef environments that relates incident hydrodynamics and coral reef geomorphology to expected runup. While the initial BEWARE database covers idealized fringing reef profiles, the BEWARE2 database captures a range of real-world reef profiles defined based on the profile characterization by *Scott et al. (2020)*. BEWARE2 was shown to accurately capture wave runup at the Fiyoaree reef profile with an RMSE of 0.21 m and bias of 0.05 m (see Supporting Information S1). Synthetic wave conditions with associated runup below 1.75 m, just below the island crest level, were excluded from the XBeach model simulations as they will not significantly influence vertical island adjustment.

2.3 Simulating the coral island's response using XBeach

The morphological response of Fiyoaree to the 80 years of synthetic wave events was simulated using XBeach, a process-based nearshore model that solves the depth-averaged, horizontal equations for flow, wave propagation and sediment transport (*Roelvink et al., 2009*). The XBeach-NH+ model was used, which solves the generation and transformation of both short and infragravity waves with an efficient reduced two-layer approach (*De Ridder et al., 2021*), enabling accurate predictions of waves and water levels across the reef and the resulting runup and flooding (*Storlazzi et al., 2018*). The XBeach-G module within XBeach-NH+ enables the computation of groundwater flow using Darcy's Law modified for turbulent flow conditions and infiltration and exfiltration through the bed (*McCall et al., 2014*). XBeach-G also allows the computation of sediment transport and storm-induced bed level change for coarse sediments (bedload only) (*McCall et al., 2015*). Here we use the formulation of *Nielsen (2002)* for sediment transport on coral island beaches, as in *Masselink et al. (2020)*.

A baseline one-dimensional XB-NH+ model was set up based on bathymetric measurements at Fares-Mathooda (a nearby island with similar characteristics to Fiyoaree for which bathymetric data were available), merged with the topographic profile of Fiyoaree. The grid resolution is high in shallow areas and on the beach to accurately simulate shallow water wave transformation and the island's morphological response. XB-NH+ parameters were adopted from *Roelvink et al. (2021)*. Reef friction values were parametrized following *Storlazzi et al. (2021)*, with friction values (c_f) of 0.05 for the reef flat, 0.1 for the fore reef and 0.003 for the beach.

The influence of five climate adaptation options was assessed by adapting the baseline XBeach model (see Figure 3 and Table 2). The strategy of restoring reefs to improve coastal protection is increasingly proposed (*Viehman et al., 2023*) and quantified (*Brathwaite et al., 2022*). Therefore, four coral restorations were designed, including three artificial coral reef structures and an ecological fore reef restoration. Artificial coral reef structures were schematized as 10 m wide and 1.25 m high bed level elevations with increased roughness (c_f of 0.15), in line with *Storlazzi et al. (2021)*. Artificial reef locations were based on *Roelvink et al. (2021)*. Ecological fore reef restoration was modeled by increasing the roughness (c_f of 0.15) across the fore reef between depths of -7 m and -1 m, the lower limit set by the operational constraints specified by *Storlazzi et al. (2021)*. We also investigated the effect of strengthening the berm crest to reduce overwash and flooding events. The berm top barrier (*Lewis, 2021*) was simulated by adjusting the initial (sandy) island crest elevation (see Figure 3). In addition, simulations with reduced roughness (c_f of 0.01) across the fore reef and reef flat allow us to explore the influence of coral degradation.

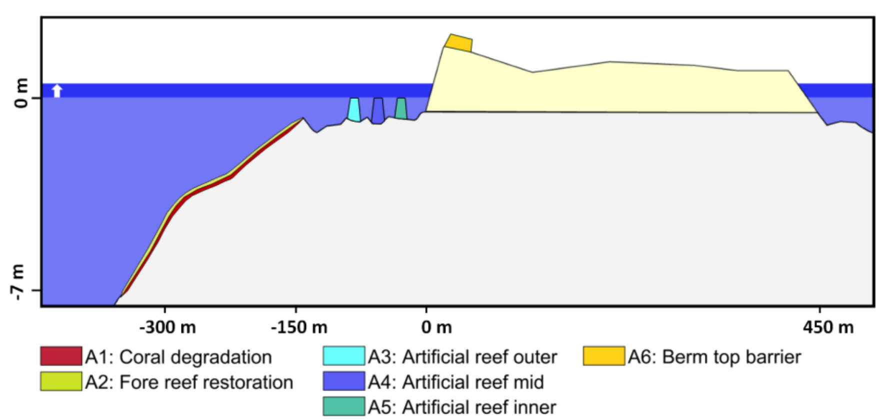

Figure 3: The coral island transect representative of Fioyaree and the potential adaptation measures. The grey area shows the immovable coral island substrate, the light yellow the movable sandy island.

Table 2: Overview of the adaptation measures included in the modelling study.

Label	Name	Description
A0	No adaptation	Baseline scenario without adaptation measures.
A1	Coral degradation	Reduced fore reef and reef flat roughness (c_f = 0.01)
A2	Fore reef restoration	Increased roughness (c_f = 0.15) across the fore reef, between -7 and -1m depth.
A3	Artificial reef outer	A 10 m wide, 1.25 m high artificial reef at the outer edge of the reef flat.
A4	Artificial reef mid	A 10 m wide, 1.25 m high artificial reef at the middle of the reef flat.
A5	Artificial reef inner	A 10 m wide, 1.25 m high artificial reef at the inner edge of the reef flat.
A6	Berm top barrier	An increase in the height of the initial berm.
[-]	Static island	Model scenario without morphological bed updating.

Calibration tests were performed to define realistic settings for the sediment transport parameterization required for the morphological bed updating. The underlying assumption is that the current island is in equilibrium with the forcing, implying that it should not change significantly during regular storms and under the present sea level. The key tuning parameters are the hydraulic conductivity K and the Nielsen phase angle ϕ for sediment transport. Sensitivity tests were performed for K values of 0, 0.0005, 0.001, 0.005 m/s, and ϕ values of 28, 30, 32, and 34°. A K value of 0.0005 m/s combined with a ϕ value of 30° gave the most stable results for the first five years of wave events without sea level rise and without extreme overwash events, and was therefore adopted for the final simulations (see Supporting Figure S2).

The 80-year time series consists of a sequence of synthetic wave events, each event described by its date of occurrence, duration, corresponding offshore water levels (the sum of the tidal water level, surge, and a sea level rise component), the wave height variation during the event, and a constant wave period (as detailed in Section 2.3). Each wave event was simulated individually, with the final bathymetric profile of one event serving as the input for the subsequent modelled event, assuming no morphological changes between separate events (waves not sufficiently energetic to reach the island crest). In total, 243 wave events were simulated, spanning a combined duration of 1114 hours. XBeach required approximately 20 to 25 minutes per simulated hour on a single node of a basic laptop.

The inundation patterns and the morphological evolution of the coral island were parametrized to assess the response of the island to sea level rise, considering different adaptation scenarios. For each wave event, the elevation and cross-shore position of the island's crest and the maximum overwash discharge were recorded. XBeach water level and velocity time series were post-processed in chunks of 1800 s to determine wave heights and water levels across the reef and the resulting runup. We used the method of *Guza et al. (1984)* to decompose the water level time series into incoming and outgoing components based on local water level elevations and current velocities. From spectral analysis, the corresponding total, incoming and outgoing wave height components were determined. A split frequency of 0.5 times the peak frequency of the incident waves was used to differentiate between sea-swell waves (denoted by SS; frequency greater than 0.5 times the peak frequency) and low-frequency waves (denoted by LF; frequency less than 0.5 times the peak frequency), as described by *Roelvink and Stive (1989)* and *Lashley et al. (2018).*

From the runup elevation time series, the $R_{2\%}$ runup levels were calculated, defined as the 2 % exceedance value of the runup peaks. To determine the different water-level contributions to the runup ($\eta_{2\%,\ runup}$) and incoming water level at the beach toe ($\eta_{2\%,\ toe}$), we also extracted the sea-swell (SS), infragravity (IG) and very low frequency (VLF) wave, and steady setup components from the runup and incoming water level elevation time series, respectively, following *Pearson et al. (2017)*. The steady setup component was calculated as the mean water level relative to the still offshore water level, while the SS, IG, and VLF wave components were obtained from the detrended runup and beach toe water level time series by spectral analysis. The total water level (relative to mean sea level) and its components were then sorted in ascending order to select the 2% exceedance value.

3 Results

3.1 Wave transformation across natural and adapted reef profiles

Figure 4 shows the wave transformation across the natural Fiyoaree coral reef profile during an energetic synthetic wave event, the third wave event in the 243-event time series. Wave transformation across this profile is characterized by shoaling across the fore reef (panels a and b in Figure 4), wave breaking across the upper fore reef and reef crest (panels b and c in Figure 4) and subsequent dissipation across the reef flat (panels c and d in Figure 4). Incident wave reflection is limited at the gently sloping (1:20) upper fore reef, while reflection of low-frequency (LF) waves (VLF and IG components) at both the fore reef and beach can be significant. Wave breaking in the relatively narrow surf zone induces a significant increase of the mean water level across the reef (setup). The time-varying location of the breakpoint is an important driver of the nearshore IG wave energy, as also observed by *Merrifield et al. (2014)* and *Becker et al. (2016)*, among others. On the inner reef flat, very-low frequency (VLF) energy peaks were observed when the LF peak frequency at the reef crest coincided with the natural resonance frequency of this reef, which is a function of the length and depth of the reef flat (*Péquignet et al., 2009*). The VLF energy peak around the fundamental resonant mode (see Supporting Figure S3) is an indication of the occurrence of resonance on this relatively narrow and smooth reef flat. A second surfzone is present near the island beach, where radiation stress forced set-down and setup can be clearly identified (not shown here).

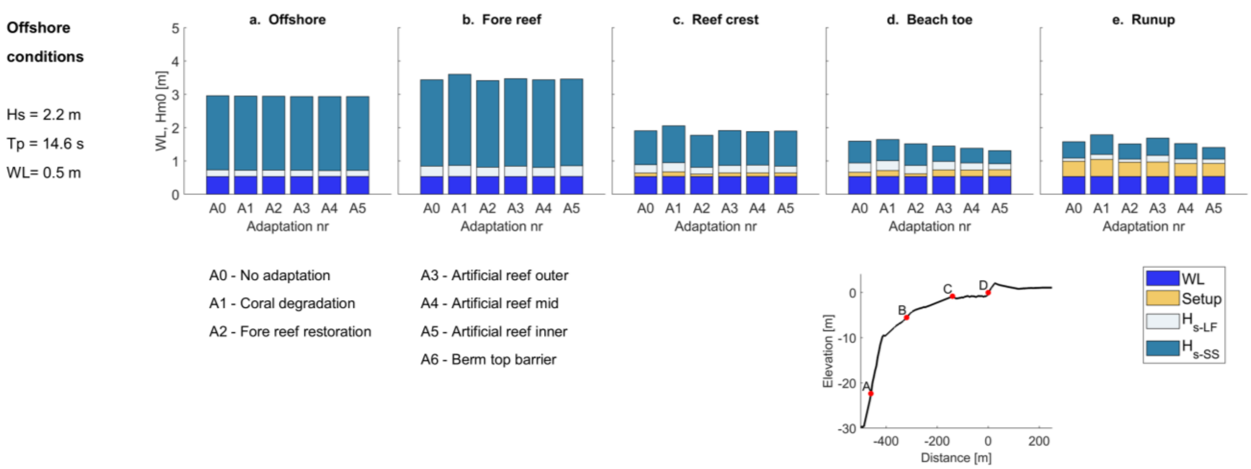

Figure 4: Wave transformation across both unrestored (A0) and adapted (A1 to A5) reef morphologies, depicting water level and total wave height components at four locations across the reef (columns; a. offshore, b. fore reef, c. reef crest, and d. beach toe) as well as the $\eta_{2\%,runup}$ (panel e) for a single synthetic wave event with a significant wave height of 2.2 m, peak wave period of 14.6 s and offshore water level of 0.5 m.

Wave transformation and setup across a reef, and the resulting runup, are highly dependent on the incident wave conditions and water levels, as stipulated by *Becker et al. (2014)* and *Pearson et al. (2017)*. Here, we investigated the influence of extrinsic conditions on the incoming water level components at the beach toe (setup, VLF, IG, and SS; Supporting Figures S4-S7) instead of the runup, as the runup levels are (more) influenced by the morphological response of the island and are curtailed by the island crest. The setup across the reef shows a strong correlation with the offshore wave power (see Supporting Figure S4), while the modelled water level variations were too small to show significant trends. VLF waves were only observed for long period incident wave conditions (T_p longer than 18 s, see Supporting Figure S5) and for reef flat water depths larger than approximately 1.4 m, during which resonant modes could be excited. The incident wave period has a significant control on the incoming IG wave heights, mainly through reflection at the fore reef. The long period incident waves generated long period LF waves at greater water depths (through intensified shoaling), in this case the steeper part of the forereef, which was likely to increase their reflection. As a result, the incoming IG wave height at the reef flat was higher for shorter period waves (see Supporting Figure S6), although the total (incoming plus outgoing) IG wave energy is higher for longer period waves due to the large reflection at the beach. The nearshore short wave energy was mainly dictated by reef flat water depths (Supporting Figure S7). Combining the wave attenuation statistics across the range of model variations during the 243 wave events, the incident wave energy is reduced by 30 to 80% at the reef crest of the unrestored reef profile (median value of 58 %; Figure 5a,c), with the percentage of energy reduction increasing with the offshore wave height (see Figure 5a). Only 5 to 20 % of the offshore wave energy reaches the shore (median value of 11 %; Figure 5b,d), and this value decreases with increasing offshore wave height (Figure 5b).

Adaptation strategies influence wave transformation by promoting wave energy dissipation through friction and wave breaking. The fore reef restoration (A2) reduces the setup (especially for low wave power events, see Supporting Figure S4) and infragravity (IG) wave heights (especially those generated during low wave period events, see Supporting Figure S6). In contrast, coral degradation (A1) decreases the dissipation of incident wave energy over the forereef, allowing more wave energy to be transmitted to the reef flat. The increase in radiation stress gradients as a result of reduced short wave dissipation amplifies the setup and breakpoint-generated low-frequency waves (Figure 4c, Figure 5c). Enhanced frictional dissipation across the fore reef reduces extreme beach toe water levels by 4 % (median; see Figure 5e) to a maximum of 12 %, while coral degradation increases extreme water levels by 5 % (median; Figure 5e).

The effectiveness of artificial reefs (A3, A4, and A5) in reducing coastal hazards is strongly dependent on their location and the prevailing forcing. Located close to the wave breaking point, the outer artificial reef structure (A3) can increase rather than decreases runup (see Figure 5e) due to the amplification of the setup and IG motions caused by the enhanced radiation stress gradients (see Supporting Figures S4 and S6), as also observed by *Roelvink et al. (2021)*. Additional setup by the artificial reef (likely overestimated in a 1D model, see Discussion) is mainly observed during low water levels and relatively low offshore wave power. The increased water level across the reef flat in turn reduces depth-induced wave breaking and frictional wave dissipation, further exacerbating the risk of flooding. The artificial reef structures closer to shore (A4 and A5) locally increase the setup but generally reduce the wave-driven contribution to runup, especially by reducing the short wave energy reaching the shore (Supporting Figure S7). Overall, the median extreme water level reductions are 6, 11, and 15% for the outer, middle, and inner artificial reef structures, respectively, with maximum reductions of almost 30% (see Figure 5e).

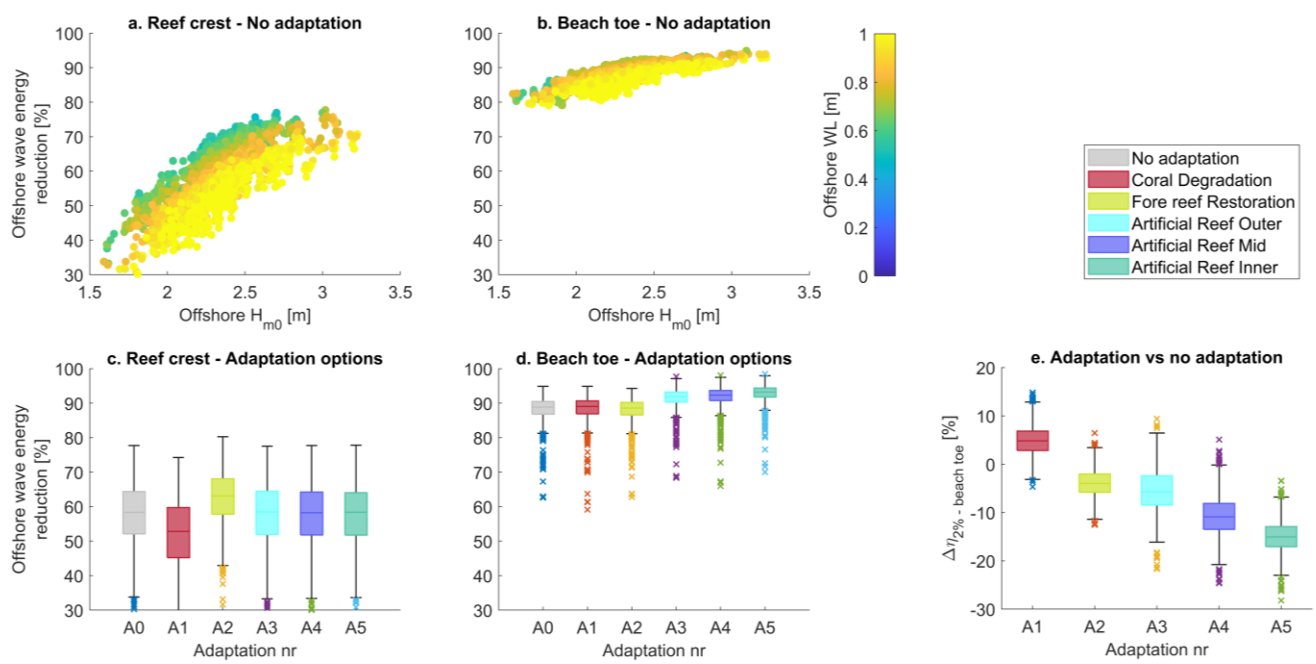

Figure 5: Offshore wave energy reduction at the reef crest (panel a) and beach toe (panel b) of the unrestored reef profile (A0), colored based on the offshore water level. Panels c and d depict offshore wave energy reduction values at the reef crest and beach toe for both unrestored (A0) and adapted (A1 to A5) reef morphologies. The reduction in extreme beach toe water levels ($\Delta\eta_{2\%}$; positive values denote an increase in extreme water levels) of adapted reefs relative to the unrestored reef is depicted in panel e. The boxplots in panels c, d, and e depict the median, lower (25%), and upper (75%) quartiles (colored boxes), the minimum and maximum values not considered outliers (black lines), and the outliers (crosses).

3.2 Morphological response of natural coral islands to SLR

The modelled response of the natural coral island beach profile over the 80-year simulation period shows significant morphological change, including profile flattening and steepening (Figure 6d), vertical accretion (Figure 6e), island retreat (Figure 6f) and crest flattening (Figure 6g). Low-energy, short-period wave events tend to flatten the lower beach profile and steepen the upper beach profile, creating a wide berm as observed by *Jackson et al. (2002)* (see Figure 6d). The inflection point between the steeper upper beach face and lower-gradient lower beach face is strongly controlled by the water level. High-energy, longer-period wave events re-steepen the beach profile to the approximate shape observed in Figure 6e–g. Limited overwash leads to vertical accretion of up to 0.1 m during a single wave event (Figure 6e), whereas there is retreat of up to 1 m during more intense wave events (Figure 6f). Figure 6c reveals the sensitive threshold between vertical accretion with and without island retreat, where a slight increase in overwash discharge induces crest retreat (compare panels e and f of Figure 6). Extreme wave events with mean overwash discharge exceeding the 10 L/m/s threshold observed by *Masselink et al. (2020)* lead to a lowering (-0.06 m) and retreat (2.5 m) of the island's crest (see Figure 6c and 6g).

As sea level rises, the island's crest gradually builds up and retreats over time (Figure 6b), as also demonstrated by *Masselink et al. (2020)*. During the first 10–15 years of wave events, the morphological adjustment of the island is limited, suggesting that the current island morphology is not in equilibrium with the forcing. It is worth noting that there is strong evidence that atoll islands in the Maldives were established during the mid-Holocene with slightly higher sea level (*Kench et al., 2005*). The implication is that these islands are somewhat 'attuned' to a sea level elevation above current sea level and this, perhaps, explains the delay in island response to SLR in the simulation. Another explanation is a slight disequilibrium in the model, and that wave runup may in reality be slightly higher than predicted, i.e., matching the current beach crest. From 2035 onwards, the island crest accretes vertically not only due to the rise in nearshore water levels, but also due to the concurrent increase in wave energy (when reef flat accumulation does not keep pace with SLR). Periods following destructive events such as a hypothetical event in 2051 (Figure 6g) are followed by accelerated crest accretion (Figure 6c), while periods following highly accretive events (Figure 6f) are followed by more mild accretion. After the high energy wave event in 2051, retreat rates are relatively constant. Over the 80-year period, the island has accreted by 0.7 m, keeping pace with the 0.5 m SLR and the concurrent increase in nearshore wave energy. However, the threshold between crest accretion and crest lowering and retreat, or even complete island rollover, is likely sensitive and could shift with higher rates of SLR or changes in storm intensity and frequency. For Fiyoaree, the assumption of a static island morphology that does not evolve with SLR (compare black and grey lines in Figure 7) leads to an increase in overwash hours by 2100 by almost a factor of three (Figure 7c). Thus, ignoring the natural morphological response of the island to sea level rise when projecting future flood risk is likely to result in an overly bleak outlook for the habitability of this island.

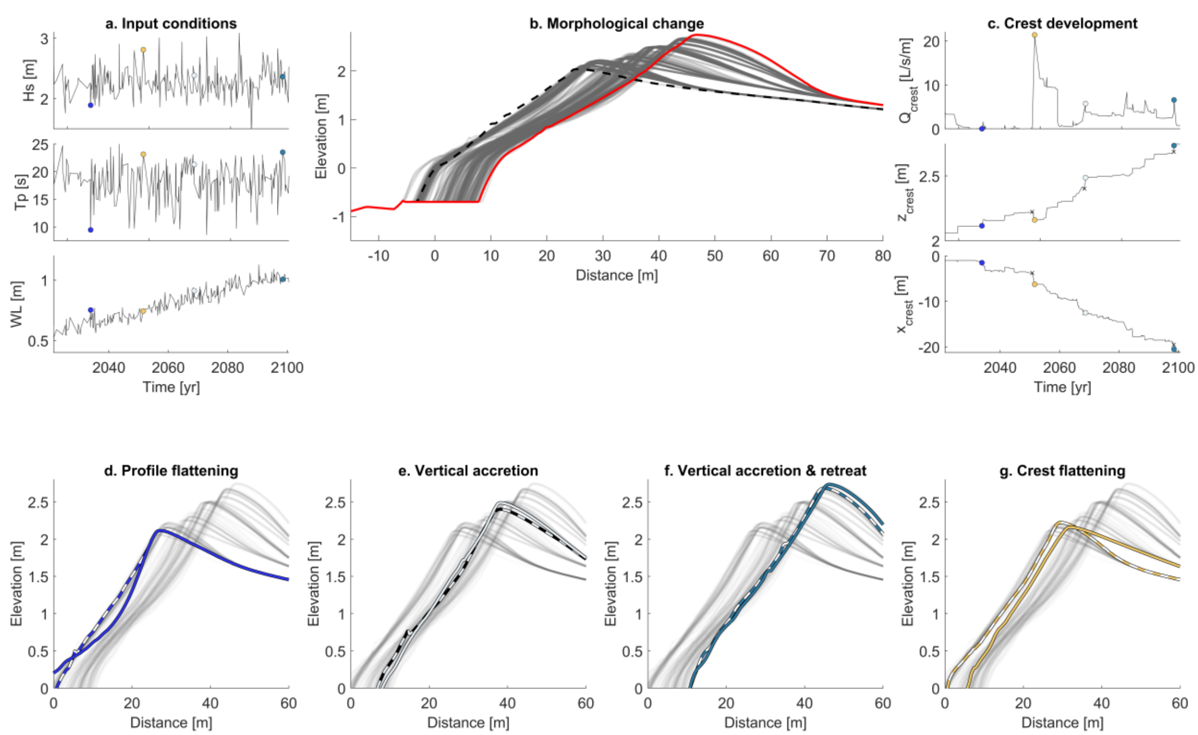

Figure 6: Morphological change of the Fiyoaree reef profile without interventions, depicting the input conditions (panel a), the resulting morphological change over time (panel b), and the development of the beach crest in terms of crest discharge, crest elevation, and cross-shore position of the crest (panel c). Panels d–g indicate different modes of the morphological response, for which the corresponding input conditions and crest development indicators are color-coded in panels a and c. Dashed, grey, and colored lines show the initial, intermediate, and final profiles, respectively.

3.3 Morphological response of reef profiles with adaptation

Figure 7 shows the projected bed levels by 2100 for the natural and adapted island simulations (grey and colored lines) and the static bed (black line) (Figure 7a), the morphological response over time in terms of crest elevation, crest retreat and hours of overwash (Figure 7b), and the projection of the morphological response and inundation for 2100 (Figure 7c). Adaptation measures either modify the nearshore wave energy (A1–A5) or limit overtopping (A6), influencing accretion and retreat rates, thereby ultimately shaping the island's morphology. Enhanced nearshore wave energy and wave setup due to coral degradation (A1) leads to large vertical accretion (*dz* = +0.8 m), but also a higher frequency of overtopping (410 hours of overwash exceeding 10 L/m/s) and retreat (*dx* = -30 m) compared to the natural profile, which experiences an accretion of +0.7 m, 320 hours of overwash, and a retreat of 21 m. In contrast, fore reef restoration reduces the overtopping frequency by 6% (290 hours of overwash exceeding 10 L/m/s) and retreat by 10% (*dx* = -19 m) compared to the natural profile, with less vertical accretion (*dz* = +0.65 m). The inner artificial reef, which is most efficient in wave height reduction, exhibits the lowest increase in crest height after 80 years of wave events (*dz* = +0.5 m), with a frequency of intense overwash (305 hours) similar to the natural profile. Given that the outer and mid artificial reef structures can amplify setup and LF motions, they do not reduce the total number of hours of more intense overwash events (Figure 7c, bottom panel). Nonetheless, they do result in lower retreat and crest accretion values. Evidently, the island crest height is in equilibrium with the nearshore wave energy level; therefore, the more energy dissipation across the fore reef and reef flat, the lower the crest elevation. The berm top barrier shows a highly variable behavior over the years. By 2065 there is hardly any overtopping and hence limited accretion (*dz* = +0.05 m) or retreat (*dx* = -4 m). The island crest has become steep and narrow in contrast to other island profiles that have accreted vertically, but that have also widened during periods of overwash. Consequently, several events around 2080 contribute to a significant crest lowering (*dz* = -0.2 m) and a large retreat (*dx* = -12 m) is observed between 2080 and 2100. The rate of retreat is strongly dependent on the initial design of the berm top barrier. Wide(r) berm enhancement works are likely to mimic the natural response of the island to SLR without flooding or island retreat.

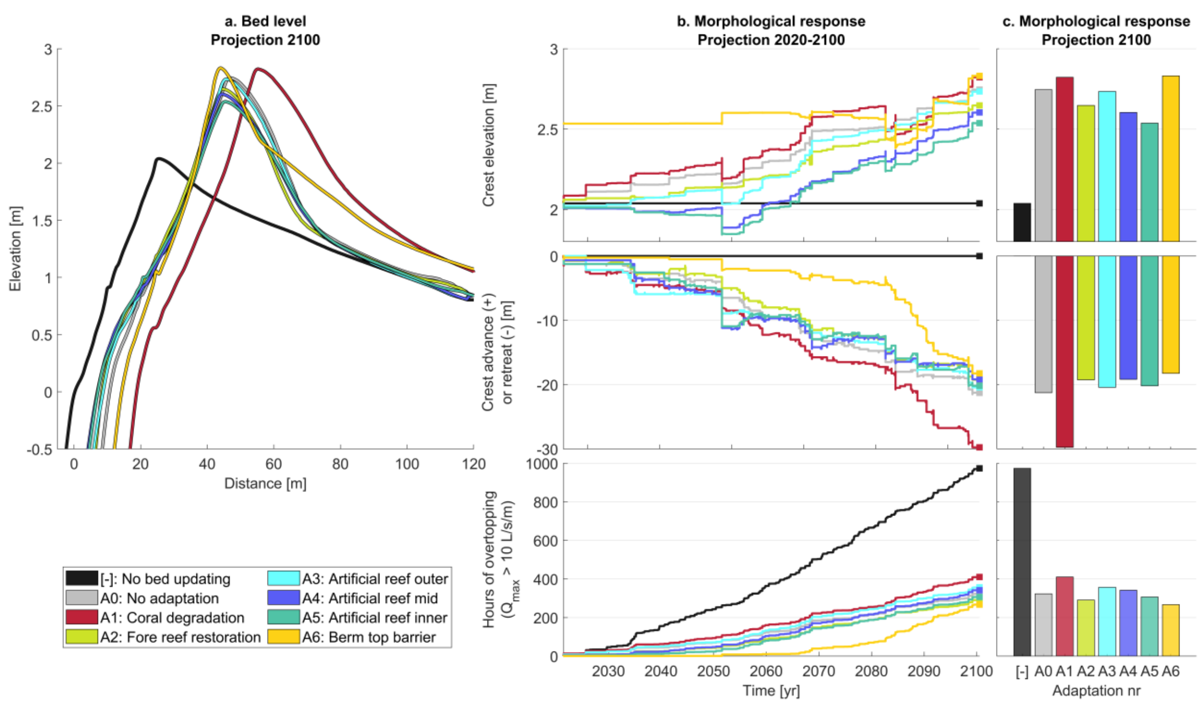

Figure 7: Modelled bed level projections for 2100 (panel a), the morphological response indicators over time (panel b), and the morphological response projection for 2100 (panel c) for the unrestored (A0) and adapted (A1 to A6) reef morphologies, as well as the static bed scenario ([-]). The morphological response is quantified by the crest elevation, crest retreat, and cumulative hours of overtopping.

Figure 8 shows the morphological response of the island, parametrized by the crest elevation change Δz_b, plotted against the extrinsic conditions (offshore wave height, wave period and water level) as well as the island freeboard (here defined as the difference between the island crest height and the extreme water level at the beach toe $\eta_{2\%, beach}$), for a subset of the adaptation scenarios. Two hypothetical extreme events resulted in significant reductions in crest height and retreat in the model: the 2051 event (see also Figure 6g and Figure 7) and the 2082 event (see also Figure 7). During the 2051 event, inundation primarily stems from extreme wave conditions (large wave height, long wave period), whereas the 2082 event is characterized by long-period waves over elevated reef flat water levels. Degraded reefs are particularly vulnerable to the 2051 and 2082 wave events, with a total reduction in crest height (sum of markers per event in Figure 8) of 0.1 m and 0.15 m respectively, in contrast to total reductions of 0.06 m and 0.01 m for the natural reef, and almost negligible change for the restored reef. Although the artificial reef structures do not perform well under the energetic wave conditions of 2051 due to the low water levels (resulting in 0.08 to 0.12 m of crest lowering), they cause only modest crest lowering in 2082. Degraded reefs experience wave events that cause crest lowering more frequently than other adaptation scenarios. Yet, there are also more instances of crest accretion, allowing vertical growth in response to SLR and the increased inshore wave energy. The difference between the island crest height and extreme beach toe water levels, indicated by the freeboard in the right panels of Figure 8, provides a first indication of the morphological response of the island. When the freeboard exceeds 0.8 m, no changes occur. Within the range of 0.5 and 0.8-m freeboard, there is a tendency for crest accretion. Below 0.5-m freeboard, the island crest generally tends to lower. The subtle variations in forcing between the 2068 and 2088 events with divergent morphodynamic response highlight the sensitivity of the threshold for crest elevation change.

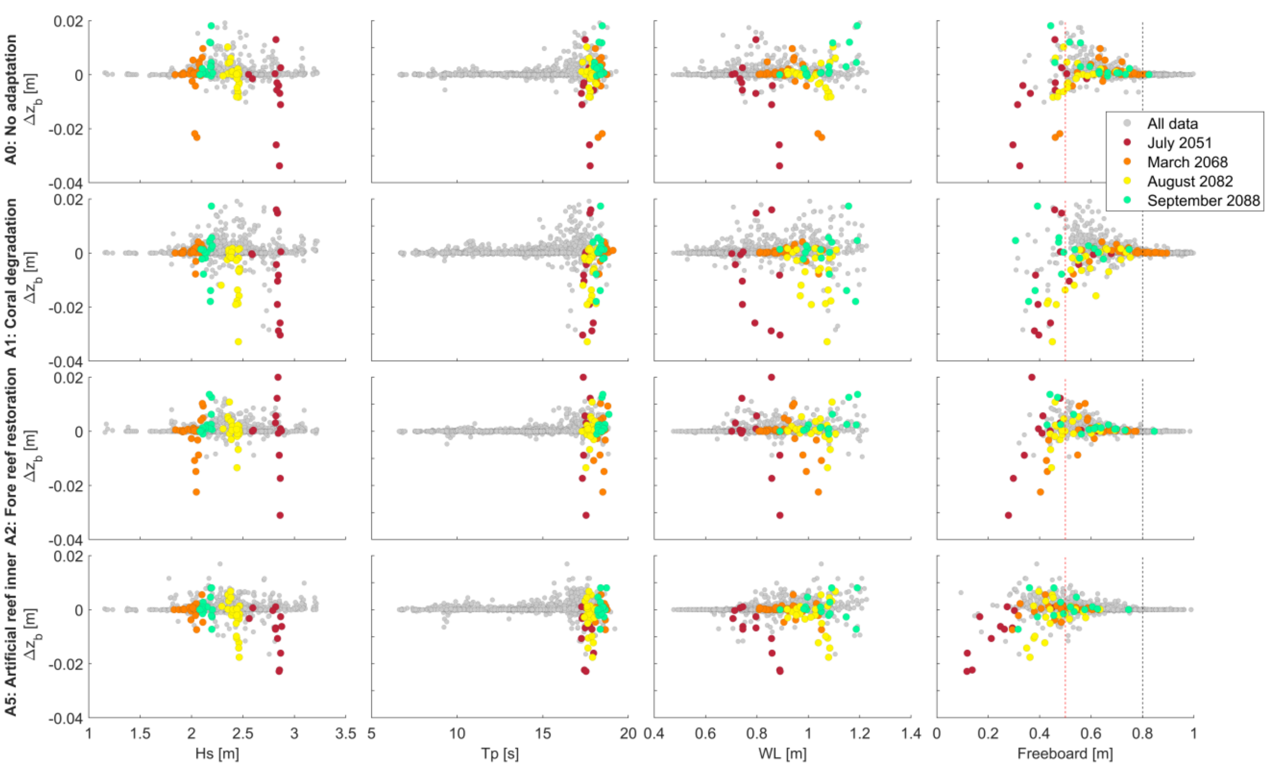

Figure 8: The crest elevation change (y-axis) at half-hourly time intervals for all wave events (grey markers) and four specific events (colored markers), plotted against the offshore wave height (H_s), wave period (T_p), and water level (WL), as well as the freeboard, which was defined as the difference between the island crest height and the extreme beach toe water level ($\eta_{2\%, beach}$). The rows depict results for four different scenarios; A0: No adaptation, A1: Coral degradation, A2: Fore reef restoration, and A5: Inner artificial reef, chosen for their distinct morphological behavior.

Discussion

Atoll islands are dynamic landforms that evolve under the influence of wind, waves, currents, and sea level (*Kench et al., 2009*) with the potential to adapt and remain habitable through overwash-induced accretion. This is true for more pristine coral island types, while on heavily urbanized islands (such as Malé), engineering solutions are often favored to maintain their functionality (*Kench et al., 2011*). In this study, we used the XBeach-NH+ model to simulate the morphological response of Fiyoaree, a sparsely populated island in the Maldives, to 80 years of synthetic wave events under SLR. Various adaptation measures, including fore reef restoration, artificial reefs on the reef flat, coral degradation, and berm restoration were examined for their influence on reef hydrodynamics and the island's morphological response. Results revealed that artificial reefs can reduce nearshore extreme water levels by 15% compared to the 'no-adaptation scenario', with a maximum reduction of approximately 30%. Enhanced frictional dissipation from fore reef restoration reduced nearshore extreme water levels by 4%, while coral degradation resulted in a 5% increase. A clear balance was observed between the wave energy reaching the toe of the island and the elevation of the island crest, with the lowest equilibrium crest heights observed for the adaptation measures most effective in attenuating wave energy. As a result, the island crest height of adapted reefs initially exceeds its equilibrium value, reducing the frequency of overwash events. However, as sea levels continue to rise, adapted islands respond morphologically through accretion and retreat. Consequently, once the islands are in equilibrium with their overwash regime (a few decades into most simulations), fairly similar future flood frequencies are projected between adapted and unrestored islands. However, adaptation measures, especially fore reef restoration, can reduce the impact of the more extreme events that lead to significant island crest lowering and retreat. Degraded reefs are particularly vulnerable to these events, showing highest levels of crest lowering and retreat for specific events. The berm top barrier provides protection with limited nuisance flooding or retreat until 2080. Its narrow design strongly influences the progressive retreat after 2080, which wider and more regular berm enhancement works may prevent.

According to the model simulations, overwash events that resulted in crest accretion were characterized by overwash discharges of less than 10 L/m/s. Higher discharges resulted in the lowering of the island crest and accretion of the island landward of the crest, agreeing with findings from previous studies (*Masselink et al., 2020; 2021*). Another indicator of island accretion is the freeboard, defined here as the difference between the island crest height and the extreme beach toe water level ($\eta_{2\%}$). Below a 0.5-m freeboard, crest lowering generally occurs, while freeboards between 0.5 and 0.8 m predominantly show accretion. Both crest accretion and island accretion are necessary to prevent the drowning of islands from SLR, although the challenges posed to island communities by the required flooding events are significant. Ignoring the morphological adaptation of the island leads to a threefold increase in the predicted inundation hours for Fiyoaree. Thus, for islands that can morphodynamically adjust to SLR, the assumption of a static island used in most climate risk studies results in a conservative estimate of future flood risk and adaptation timescales. However, given the computational expense of running advanced morphodynamic models, it is necessary to either to accelerate these models or to parametrize the island adjustment to sea level rise if they are to be included in large-scale flood risk assessments.

This study presents a methodological approach for long-term process-based modelling to gain further insight into the future coastal flood risk of coral islands. The study is limited by both hydrodynamic and morphodynamic model assumptions and schematizations. One-dimensional reef models, for instance, do not account for two-dimensional effects such as (artificial reef-induced) horizontal circulation cells and longshore currents, which can play a critical role in balancing wave-induced setup with offshore flow (e.g., *Lowe et al., 2010*). Additionally, wave interactions resulting in energy transfer to low-frequency waves are overestimated in a 1D approach (e.g., *Herbers et al., 1994*). However, these limitations do not detract from the primary focus of this paper which addresses the relative comparison of flood risk, rather than the absolute representation of flood risk, for different adaption strategies. Morphodynamic model limitations are related to the computation of sediment transport with the XBeach-gravel module, which is highly dependent on the hydraulic conductivity and Nielsen parameter, and these have been poorly validated for smaller sediment sizes (*Masselink et al., 2020*). Additional experiments should inform on the accuracy of the morphological response of coral islands.

In terms of model schematization, there are limitations related to the representation of artificial reefs and the berm top barrier, as well as in the schematization of the wave climate. Artificial reefs were modelled as impermeable bed level elevations with enhanced roughness, following *Roelvink et al. (2021)*. This approach does not account for flow through the structure, leading to an overestimation of the wave height reduction, the setup, and of the reflection at the structure, both for incident waves reflected offshore and for waves reflected from the beach towards the structure and back. The overestimation of the setup across the structure, combined with the general overestimation of setup in a 1D model, leads to underperformance of the structures in the model compared to their performance in real-world conditions during energetic wave events. Flume, wave basin, and field experiments can help to determine the most effective approaches to modelling these structures with XBeach. The effectiveness of the berm top barrier is strongly influenced by its initial design. The current design included a relatively steep island crest, which subsequently led to substantial morphological adjustments when overwash events occurred compared to the wider, unrestored island crest. Finally, a single realization of wave event sequences was made. The final island profile and flood frequency could be significantly influenced by the specific sequence of wave events, not explored here because of computational limitations.

The ability of coral islands to adapt to SLR is strongly influenced by the rate and total amount of SLR. The modelled SLR of 0.5 m by 2100, assuming a constant SLR rate of 6.25 mm/yr, represents the median prediction for an intermediate emission scenario (SSP2-4.5). At higher rates of SLR (3.7 mm/yr SLR has already been observed between 2006 and 2018; *IPCC, 2021*), islands may not be able to keep up with SLR, leading to a rapid rollover and destruction of the island (*Masselink et al., 2020*). Furthermore, for higher sea levels, especially when combined with limited reef flat accumulation due to coral degradation, the reef coast will be exposed to greatly increased wave energy (e.g., *Merrifield et al., 2014*), rendering the islands highly vulnerable to extreme events. The impact of SLR rates on coral island morphology is likely to be influenced by adaptation measures. Artificial reefs may provide better protection at higher SLR rates compared to fore reef restoration, as they are most efficient at attenuating wave energy, especially for larger water depths. Therefore, they require less morphological updating of the island to achieve its equilibrium crest height, minimizing the risk of extreme overwash conditions. These considerations highlight the vulnerability of coral islands and emphasize the need to consider different rates of SLR, vertical reef growth scenarios, and adaptation measures to fully assess the potential impacts of sea-level rise on these ecosystems and coastal communities.

Coral islands rely on sufficient sediment supply to maintain their footprint. However, future sediment supply, governed by the complex interplay of ecological and physical processes (*Kench et al., 2009*; *Tuck et al., 2021*), is highly uncertain and depends on, among other things, storm climate, oceanic conditions, and the activity of bio-eroding (e.g., parrotfish; *Perry et al., 2015*) and bio-producing (e.g., foraminefara; *Dawson et al., 2014*) organisms. In addition, sediment supply from the reef system to the island can vary considerably over time and varies between islands. For example, following storm or coral bleaching events, large pulses of sediment may be transported towards the island, possibly followed by periods of low sediment supply. In the current model setup, no sediment source is introduced to the reef flat, thus ignoring changes in island sediment volume and potentially overestimating island retreat.

The morphological adjustment of coral islands to sea level rise through frequent flooding poses significant ecological challenges and impacts. Flooding can have severe ecological impacts, including the disruption of freshwater availability on the island (*Storlazzi et al., 2018*) and the destruction of agricultural activities (e.g., *Zahir et al., 2006*). Effective reef management is essential to preserve and restore crucial ecosystem services provided by coral reefs, such as protection from storms and erosion, food provision, and income generation. In addition to reducing carbon emissions, this entails adopting local measures to manage solid waste disposal, minimizing nutrient and sediment-rich runoff, controlling siltation from dredging activities, and eliminating destructive fishing practices (e.g., *Mcleod et al., 2019*). For restoration, it is important to select suitable coral reef species that can withstand elevated temperatures and increased acidity. Examples of this include porites, a coral species found on the shallow reef flat and in the warm, shallow inter-island channels of Fioyaree.

To ensure the continued habitation of atoll islands that naturally adjust to sea level rise through overwash-induced accretion, flexibility and adaptability are required of both the island infrastructure and its communities. Flexible infrastructure can be achieved through a variety of measures, such as building houses on stilts (*Esteban et al., 2019*), flood protection at the household level (raising doorstep levels, implementing local flood walls; *Brown et al., 2020*), and nature-based coastal protection measures (*Barnett et al., 2022*). Social adaptation is also a key factor in allowing for natural island dynamics. An integral part of this adaptation is the implementation of early warning systems, to enable island inhabitants to prepare effectively for potential flooding events (*Winter et al., 2020; Hoeke et al., 2021*). Allowing for natural island dynamics seems feasible in the context of the Maldives (except for the northernmost atolls), with its relatively consistent wave climate and lack of catastrophic cyclones (*Wadey et al., 2017*). Other island communities may face different challenges, particularly in parts of the Pacific where cyclones can destroy entire islands (*Ford et al., 2014*). Nevertheless, if embraced and implemented by local communities, allowing for natural island dynamics could potentially extend the habitability of islands in the Maldives beyond current projections.

Acknowledgments

This research was funded by a UKRI grant EP/X029506/1 awarded to Gerd Masselink. All data (numerical model input files and raw output files) in the study are publicly available at the Zenodo repository via https://doi.org/10.5281/zenodo.10495462 *(Roelvink, 2024)*. The XBeach software is freely available at *download.deltares.nl/xbeach*.

References

Akaike, H. (1974). A new look at the statistical model identification. IEEE transactions on automatic control, 19(6), 716-723.
Amores, A., Marcos, M., Pedreros, R., Le Cozannet, G., Lecacheux, S., Rohmer, J., ... & Khaleel, Z. (2021). Coastal flooding in the Maldives induced by mean sea-level rise and wind-waves: from global to local coastal modelling. Frontiers in Marine Science, 8, 665672.
Barnett, J., Jarillo, S., Swearer, S. E., Lovelock, C. E., Pomeroy, A., Konlechner, T., ... & Lowe, R. (2022). Nature-based solutions for atoll habitability. Philosophical Transactions of the Royal Society B, 377(1854), 20210124.
Becker, J. M., Merrifield, M. A., & Ford, M. (2014). Water level effects on breaking wave setup for Pacific Island fringing reefs. *Journal of Geophysical Research: Oceans*, *119*(2), 914-932.
Becker, J. M., Merrifield, M. A., & Yoon, H. (2016). Infragravity waves on fringing reefs in the tropical Pacific: Dynamic setup. *Journal of Geophysical Research: Oceans*, *121*(5), 3010-3028.
Beetham, E., & Kench, P. S. (2018). Predicting wave overtopping thresholds on coral reef-island shorelines with future sea-level rise. Nature communications, 9(1), 3997.
Brathwaite, A., Clua, E., Roach, R., & Pascal, N. (2022). Coral reef restoration for coastal protection: Crafting technical and financial solutions. Journal of Environmental Management, 310, 114718.
Brown, S., Wadey, M. P., Nicholls, R. J., Shareef, A., Khaleel, Z., Hinkel, J., ... & McCabe, M. V. (2020). Land raising as a solution to sea-level rise: An analysis of coastal flooding on an artificial island in the Maldives. *Journal of Flood Risk Management*, *13*, e12567.
Dawson, J. L., Smithers, S. G., & Hua, Q. (2014). The importance of large benthic foraminifera to reef island sediment budget and dynamics at Raine Island, northern Great Barrier Reef. *Geomorphology*, *222*, 68-81.
De Ridder, M. P., Smit, P. B., van Dongeren, A. R., McCall, R. T., Nederhoff, K., & Reniers, A. J. (2021). Efficient two-layer non-hydrostatic wave model with accurate dispersive behaviour. Coastal Engineering, 164, 103808.
Duvat, V. K., & Pillet, V. (2017). Shoreline changes in reef islands of the central Pacific: Takapoto Atoll, northern Tuamotu, French Polynesia. Geomorphology, 282, 96-118.
East, H. K., Perry, C. T., Kench, P. S., & Liang, Y. (2016). Atoll-scale comparisons of the sedimentary structure of coral reef rim islands, Huvadhu Atoll, Maldives. Journal of Coastal Research, (75), 577-581.
East, H. K., Perry, C. T., Kench, P. S., Liang, Y., & Gulliver, P. (2018). Coral reef island initiation and development under higher than present sea levels. Geophysical Research Letters, 45(20), 11-265.
Esteban, M., Jamero, M. L., Nurse, L., Yamamoto, L., Takagi, H., Thao, N. D., ... & Shibayama, T. (2019). Adaptation to sea level rise on low coral islands: Lessons from recent events. *Ocean & coastal management*, *168*, 35-40.
EurOtop, Van der Meer, J. W., Allsop, N. W. H., Bruce, T., De Rouck, J., Kortenhaus, A., Pullen, T. et al. (2018). Manual on wave overtopping of sea defences and related structures. An overtopping manual largely based on European research, but for worldwide application. Retrieved from www.overtopping-manual.com
Ford, M. R., & Kench, P. S. (2014). Formation and adjustment of typhoon-impacted reef islands interpreted from remote imagery: Nadikdik Atoll, Marshall Islands. *Geomorphology*, *214*, 216-222.

Guza, R. T., Thornton, E. B., & Holman, R. A. (1984). Swash on steep and shallow beaches. In Coastal Engineering 1984 (pp. 708-723).
Herbers, T. H. C., Elgar, S., & Guza, R. T. (1994). Infragravity-frequency (0.005–0.05 Hz) motions on the shelf. Part I: Forced waves. *Journal of Physical Oceanography*, *24*(5), 917-927.
Hersbach, H., Bell, B., Berrisford, P., Hirahara, S., Horányi, A., Muñoz‐Sabater, J., ... & Thépaut, J. N. (2020). The ERA5 global reanalysis. Quarterly Journal of the Royal Meteorological Society, 146(730), 1999-2049.
Hoeke, R. K., Damlamian, H., Aucan, J., & Wandres, M. (2021). Severe flooding in the atoll nations of Tuvalu and Kiribati triggered by a distant Tropical Cyclone Pam. *Frontiers in Marine Science*, *7*, 539646.
IPCC, 2021: Summary for Policymakers. In: Climate Change 2021: The Physical Science Basis. Contribution of Working Group I to the Sixth Assessment Report of the Intergovernmental Panel on Climate Change [Masson-Delmotte, V., P. Zhai, A. Pirani, S.L. Connors, C. Péan, S. Berger, N. Caud, Y. Chen, L. Goldfarb, M.I. Gomis, M. Huang, K. Leitzell, E. Lonnoy, J.B.R. Matthews, T.K. Maycock, T. Waterfield, O. Yelekçi, R. Yu, and B. Zhou (eds.)].
Jackson, N. L., Nordstrom, K. F., Eliot, I., & Masselink, G. (2002). 'Low energy'sandy beaches in marine and estuarine environments: a review. Geomorphology, 48(1-3), 147-162.
Jennath, A., Krishnan, A., Paul, S. K., & Bhaskaran, P. K. (2021). Climate projections of sea level rise and associated coastal inundation in atoll islands: Case of Lakshadweep Islands in the Arabian Sea. Regional Studies in Marine Science, 44, 101793.
Kench, P. S., McLean, R. F., & Nichol, S. L. (2005). New model of reef-island evolution: Maldives, Indian Ocean. *Geology*, *33*(2), 145-148.
Kench, P.S., Perry, C.T., Spencer, T., (2009). Coral Reefs. Chapter 7. In: Slaymaker, O., Spencer, T., Embleton-Hamann, C. (Eds.), Geomorphology and Global Environmental Change. Cambridge University Press, Cambridge, pp. 180–21
Kench, P. S. (2012). Compromising reef island shoreline dynamics: legacies of the engineering paradigm in the Maldives. In Pitfalls of shoreline stabilization: selected case studies (pp. 165-186). Dordrecht: Springer Netherlands.
Land and Marine Environmental Resources Group (LAMER) (2013). Environment impact assessment for flood mitigation and reclamation works at Fares-Maathoda, Gdh Atoll. Male': Maldives. http://saruna.mnu.edu.mv/jspui/handle/123456789/4114
Lashley, C. H., Roelvink, D., van Dongeren, A., Buckley, M. L., & Lowe, R. J. (2018). Nonhydrostatic and surfbeat model predictions of extreme wave run-up in fringing reef environments. Coastal Engineering, 137, 11-27.
Lewis (2021). Nanumea Detailed Design Report: Tuvalu Coastal Adaptation Project. Report No: P19012_DetailedDesign_NMA_R1.00. https://www.adaptation-undp.org/sites/default/files/resources/nma_detaileddesign_r1.00wapps.pdf
Lloyd, S. (1982). Least squares quantization in PCM. IEEE transactions on information theory, 28(2), 129-137.
Lowe, R. J., Hart, C., & Pattiaratchi, C. B. (2010). Morphological constraints to wave‐driven circulation in coastal reef‐lagoon systems: A numerical study. *Journal of Geophysical Research: Oceans*, *115*(C9).
Luijendijk, A. P., de Schipper, M. A., & Ranasinghe, R. (2019). Morphodynamic acceleration techniques for multi-timescale predictions of complex sandy interventions. *Journal of marine science and engineering*, *7*(3), 78.
Masselink, G., Austin, M., Scott, T., Poate, T. and Russell, P. (2014). Role of wave forcing, storms and NAO in outer bar dynamics on a high-energy, macro-tidal beach. Geomorphology, 226, 76-93.
Masselink, G., Beetham, E., & Kench, P. (2020). Coral reef islands can accrete vertically in response to sea level rise. Science Advances, 6(24), eaay3656.
Masselink, G., McCall, R., Beetham, E., Kench, P., & Storlazzi, C. (2021). Role of future reef growth on morphological response of coral reef islands to sea‐level rise. Journal of Geophysical Research: Earth Surface, 126(2), e2020JF005749.
McCall, R. T., Masselink, G., Poate, T. G., Roelvink, J. A., Almeida, L. P., Davidson, M., & Russell, P. E. (2014). Modelling storm hydrodynamics on gravel beaches with XBeach-G. Coastal Engineering, 91, 231-250.
McCall, R. T., Masselink, G., Poate, T. G., Roelvink, J. A., & Almeida, L. P. (2015). Modelling the morphodynamics of gravel beaches during storms with XBeach-G. Coastal Engineering, 103, 52-66.

Mcleod, E., Anthony, K. R., Mumby, P. J., Maynard, J., Beeden, R., Graham, N. A., ... & Tamelander, J. (2019). The future of resilience-based management in coral reef ecosystems. *Journal of environmental management*, *233*, 291-301.
Merrifield, M. A., Becker, J. M., Ford, M., & Yao, Y. (2014). Observations and estimates of wave-driven water level extremes at the Marshall Islands. Geophysical Research Letters, 41(20), 7245-7253.
Nelsen, R. B. (2007). An introduction to copulas. Springer Science & Business Media.
Nielsen, P. (2002). Shear stress and sediment transport calculations for swash zone modelling. Coastal Engineering, 45(1), 53-60.
Pearson, S. G., Storlazzi, C. D., Van Dongeren, A. R., Tissier, M. F. S., & Reniers, A. J. H. M. (2017). A Bayesian-based system to assess wave-driven flooding hazards on coral reef-lined coasts. Journal of Geophysical Research: Oceans, 122(12), 10099-10117.
Péquignet, A. C. N., Becker, J. M., Merrifield, M. A., & Aucan, J. (2009). Forcing of resonant modes on a fringing reef during tropical storm Man-Yi. *Geophysical Research Letters*, *36*(3).
Perry, C. T., Kench, P. S., O'Leary, M. J., Morgan, K. M., & Januchowski-Hartley, F. (2015). Linking reef ecology to island building: Parrotfish identified as major producers of island-building sediment in the Maldives. *Geology*, *43*(6), 503-506.
Poelhekke, L., Jäger, W. S., Van Dongeren, A., Plomaritis, T. A., McCall, R., & Ferreira, Ó. (2016). Predicting coastal hazards for sandy coasts with a Bayesian Network. Coastal Engineering, 118, 21-34.
Quataert, E., Storlazzi, C., Van Rooijen, A., Cheriton, O., & Van Dongeren, A. (2015). The influence of coral reefs and climate change on wave-driven flooding of tropical coastlines. Geophysical Research Letters, 42(15), 6407-6415.
Quataert, E., Storlazzi, C., van Dongeren, A., & McCall, R. (2020). The importance of explicitly modelling sea-swell waves for runup on reef-lined coasts. *Coastal Engineering*, *160*, 103704.
Roelvink, J. A., & Stive, M. J. F. (1989). Bar-generating cross-shore flow mechanisms on a beach. *Journal of Geophysical Research: Oceans*, *94*(C4), 4785-4800.
Roelvink, D., Reniers, A., Van Dongeren, A. P., De Vries, J. V. T., McCall, R., & Lescinski, J. (2009). Modelling storm impacts on beaches, dunes and barrier islands. Coastal engineering, 56(11-12), 1133-1152.
Roelvink, F. E., Storlazzi, C. D., Van Dongeren, A. R., & Pearson, S. G. (2021). Coral reef restorations can be optimized to reduce coastal flooding hazards. Frontiers in Marine Science, 8, 653945.
Roelvink, F. E. (2024). XBeach morphological modelling Maldives (Version 1) [Data set]. Zenodo. https://doi.org/10.5281/zenodo.10495462
Rousseeuw, P. J. (1987). Silhouettes: a graphical aid to the interpretation and validation of cluster analysis. Journal of computational and applied mathematics, 20, 53-65.
Scott, F., Antolinez, J. A., McCall, R., Storlazzi, C., Reniers, A., & Pearson, S. (2020). Hydro-morphological characterization of coral reefs for wave runup prediction. Frontiers in Marine Science, 7, 361.
Smithers, S. G., & Hoeke, R. K. (2014). Geomorphological impacts of high-latitude storm waves on low-latitude reef islands—Observations of the December 2008 event on Nukutoa, Takuu, Papua New Guinea. Geomorphology, 222, 106-121.
Storlazzi, C. D., Gingerich, S. B., Van Dongeren, A. P., Cheriton, O. M., Swarzenski, P. W., Quataert, E., ... & McCall, R. (2018). Most atolls will be uninhabitable by the mid-21st century because of sea-level rise exacerbating wave-driven flooding. Science advances, 4(4), eaap9741.
Storlazzi, C. D., Reguero, B. G., Cumming, K. A., Cole, A. D., Shope, J. B., Gaido L, C., ... & Beck, M. W. (2021). Rigorously valuing the coastal hazard risks reduction provided by potential coral reef restoration in Florida and Puerto Rico: U.S. Geological Survey Open-File Report 2021–1054, 35 p., https://doi.org/10.3133/ ofr20211054
Tuck, M. E., Kench, P. S., Ford, M. R., & Masselink, G. (2019a). Physical modelling of the response of reef islands to sea-level rise. Geology, 47(9), 803-806.
Tuck, M. E., Ford, M. R., Masselink, G., & Kench, P. S. (2019b). Physical modelling of reef island topographic response to rising sea levels. Geomorphology, 345, 106833.
Tuck, M. E., Ford, M. R., Kench, P. S., & Masselink, G. (2021). Sediment supply dampens the erosive effects of sea-level rise on reef islands. Scientific Reports, 11(1), 5523.
van Ormondt, M., van Dongeren, A., & Roelvink, D. (2021). A semi-empirical method for computing storm surges on open coasts during tropical cyclones. Coastal Engineering, 165, 103839.

Viehman, T. S., Reguero, B. G., Lenihan, H. S., Rosman, J. H., Storlazzi, C. D., Goergen, E. A., ... & Hench, J. L. (2023). Coral restoration for coastal resilience: Integrating ecology, hydrodynamics, and engineering at multiple scales. Ecosphere, 14(5), e4517.
Vitousek, S., Barnard, P. L., Fletcher, C. H., Frazer, N., Erikson, L., & Storlazzi, C. D. (2017). Doubling of coastal flooding frequency within decades due to sea-level rise. Scientific reports, 7(1), 1-9.
Wadey, M., Brown, S., Nicholls, R. J., & Haigh, I. (2017). Coastal flooding in the Maldives: an assessment of historic events and their implications. Natural Hazards, 89, 131-159.
Winter, G., Storlazzi, C., Vitousek, S., Van Dongeren, A., McCall, R., Hoeke, R., ... & Wandres, M. (2020). Steps to develop early warning systems and future scenarios of storm wave-driven flooding along coral reef-lined coasts. Frontiers in Marine Science, 7, 199.
Zahir, H., Allison, W., Dews, G., Gunn, J., Rajasuriya, A., Luc Solandt, J., ... & Wakeford, M. (2006). Post-tsunami status of the coral reefs of the islands and atolls of the Maldives. In Wilkinson, C., Souter, D. & Goldberg, J. (Eds.) , Status of Coral reefs in Tsunami affected countries : 2005 (pp. 111-123)). http://saruna.mnu.edu.mv/jspui/handle/123456789/4377